

Growth modes depending on the growing temperature in heteroepitaxy: Au/Ni(111)

Kenji Umezawa* and Shigemitsu Nakanishi

Department of Materials Sciences, University of Osaka Prefecture, Sakai, Osaka 599-8531, Japan

Walter M. Gibson

Department of Physics, University at Albany, SUNY, 1400 Washington Avenue, Albany, New York 12222

(Received 12 January 1998)

The growth of multilayers of Au atoms on Ni(111) has been mainly investigated by using time-of-flight-type impact-collision ion-scattering spectroscopy. We found that only two different types of epitaxial growth exist: Au[11 $\bar{2}$]||Ni[11 $\bar{2}$] (normal mode) and Au[$\bar{1}\bar{1}2$]||Ni[11 $\bar{2}$] (reverse mode). Moreover, the relative amount of these two growths show an observed oscillatory dependence on the growing temperature during deposition. It is found that the energetics and dynamics of the second layer of Au atoms control this behavior during deposition. [S0163-1829(98)00816-9]

The growth of metals on metal surfaces is considerably more complex and interesting than expected from simple macroscopic considerations. Recent advances in experimental epitaxial growth techniques have greatly enhanced the capability to grow artificially structured materials.¹ The growth mode of heteroepitaxial systems is determined by a detailed balance between the structure of the bulk phases of two different materials and interatomic interactions at the interface.^{2,3} Layer-by-layer growth can be induced by creating an enhanced density of nuclei during the early stage of growth of each monolayer. Recently the growth mode in heteroepitaxy has been controlled by temperature reduction during nucleation and pulsed ion beam bombardment during deposition.³ Also surfactant-mediated epitaxial growth has attracted increasing interest in recent years.⁴ Experimental methods like scanning tunneling microscopy (STM) and low-energy electron diffraction (LEED) have made it possible to study the arrangement of the atoms during the growth of a metal on metal. Among various methods for surface structure analysis, ion scattering spectroscopy is a unique real-space method in which the Newtonian scattering of a classical particle—an ion—is used. Low-energy ion scattering with backscattering close to 180° has been used to determine the surface structure of single crystals in a direct way. Especially, impact collision ion scattering spectroscopy (ICISS) with time-of-flight (TOF) detection allows one to easily analyze the atomic structure of solid surfaces. Difficulties arising from the ion beam neutralization effect of noble gases can be excluded since a TOF-ICISS system can detect both neutrals and ions scattered from surfaces by using a microchannel plate (MCP).⁵⁻⁸ One or two atomic layers near the surface as well as surfaces below several atomic layers can be “seen.”

There have been many structured studies of metals adsorbed on fcc(111) surfaces and one of the most studied is Ni(111).⁹⁻¹² Au/Ni superlattice films have been investigated for more than 20 years.^{13,14} The Au/Ni(111) phase is a large lattice-mismatched combination (16%); the nearest-neighbor distances of bulk Au(111) and Ni(111) are 2.88 and 2.49 Å, respectively. Elemental Au-Ni is immiscible in the bulk.¹⁵ One would therefore expect that deposited Au atoms simply

grow on top of a surface of Ni. However, this is not generally the case. The TOF-ICISS method complements microscopic STM studies in that it averages over the surface and can give a reliable statistical sampling of simultaneous and competing growth modes. Jacobsen and co-workers proposed from STM studies that the growth of one monolayer of Au on Ni(111) results in an ordered array of triangular misfit dislocation loops in the underlying Ni surface.¹⁶ In this report, we present detailed TOF-ICISS results showing that when 3 ML of Au are deposited on a Ni(111) surface, an unusual heteroepitaxial growth behavior result. Two simple, symmetric growth modes dominate the ordered heteroepitaxy but the relative abundance of these two modes exhibits a striking and previously unobserved oscillatory dependence on substrate temperature during deposition. It is furthermore shown that this behavior is controlled by the energetics and dynamics of the second layer of Au atoms during deposition.

The experimental procedures described here were performed in an ultrahigh vacuum (UHV) systems with LEED, Auger electron spectroscopy (AES), and TOF-ICISS facilities. Since the details of the sample preparation and analysis are provided in earlier publications, only an outline is given in this report.^{8,11} A Ni(111) ($\phi = 12 \times 0.5$ mm thickness) single crystal was mounted on a standard *xyz* manipulator and cleaned *in situ* by repeated cycles of 500 eV-Ar⁺ bombardment followed by annealing at 800 °C to remove the surface damage until no contamination could be detected by using AES and ICISS. From ICISS measurements on the Ni substrate, we are sure that a Ni substrate is not twinned. If a clean sample is twinned, we can easily know it by polar scans of an ICISS study. Thus a sharp unreconstructed 1×1 pattern was observed by LEED. Au of 99.999% purity was evaporated at a rate of about 0.08 ML/min onto the Ni(111) crystal to a coverage of 3 ML at various substrate temperatures from RT through 675 K. The ICISS spectra were taken by chopping the primary 2 keV-Ne⁺ beam and the 180° backward scattering particles after free flight through a drift tube of 60 cm, and were detected by a MCP that was coaxially mounted along the primary tube. Polar angle scans were performed from -85° to +85° in 2° increments with an average pulsed beam current of 3–5 pA.

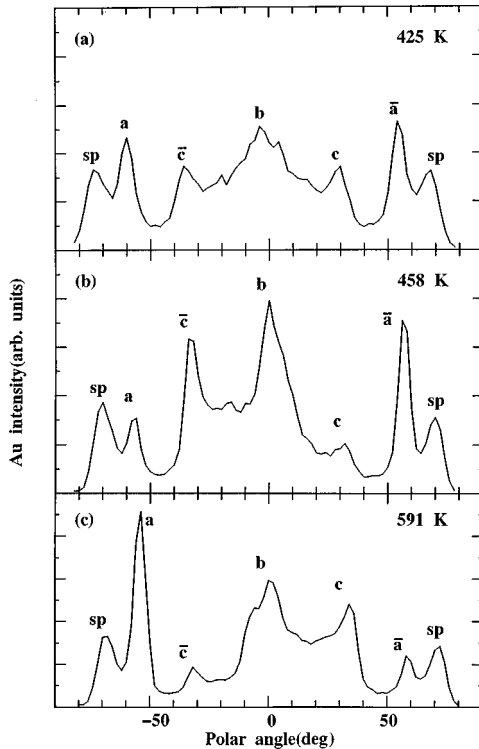


FIG. 1. A series of TOF-ICISS polar scans for 2 keV-Ne⁺ ions backscattered from Au atoms at a coverage of 3 ML along the $[1\bar{1}\bar{2}]$ azimuth. The polar angle was measured from the surface of the specimen. The ratio of type *n* and type *r* is around (a) 50 and 50%, (b) 20 and 80%, and (c) 90 and 10%, respectively.

The Au coverage was verified by Rutherford backscattering (RBS) measurements using 2 MeV-He⁺ ions. A silicon surface barrier detector with a 31.1 m sr. solid angle was located at 164° from the incident beam. The Au concentration 4.2×10^{15} atoms/cm² deduced from RBS measurements was in good agreement with the value of 3 ML obtained from TOF-ICISS analysis.

After depositing Au at a coverage of about 1.0 ML at RT, the LEED pattern was close to the 9×9 structure with respect to the underlying Ni lattice.¹⁵ Figure 1 shows a typical example of a series of ICISS polar angle scans from 3 ML of Au atoms deposited at different substrate temperatures onto Ni(111) along the $[1\bar{1}\bar{2}]$ azimuths. It clearly shows that the spectra of the polar angle scans change depending on the substrate temperature during Au deposition. The ICISS peak intensity, in general, is strongly enhanced by focusing effects in the scattering process of the incident ion beams. We can therefore explain all observed peaks as focusing effects by several specific incident directions of 2 keV-Ne⁺ beams for the Au atoms. Figure 2 shows the results of simulations based on the three-dimensional cross section for ions that scatter sequentially and classically from two atoms. This figure reproduced as well the experimental results shown in Fig. 1(a). In this simulation, we assumed that the surface structure were formed by two different domains as we describe below. There is a discrepancy seen between the simulation and the experiment at the polar angles below $\pm 58^\circ$. These features are attributed to out-of-plane scattering events. The simulations are based on in-plane scattering only within planes of atoms that represent discrete slices of the three-dimensional structure.

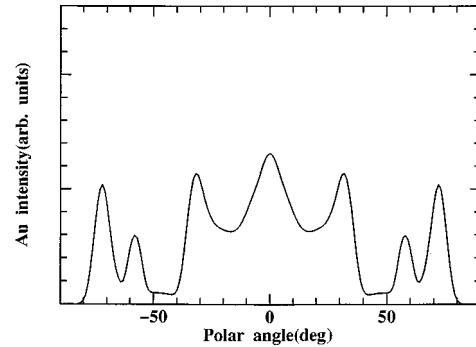


FIG. 2. The results of simulations for Au scattering intensity from the surface structure along the $[1\bar{1}\bar{2}]$ azimuth. It shows that the mixed domain of 50% each of the normal and the reverse modes exist.

We divide the observed peaks shown in Fig. 1 into two groups; one group labeled *a*, *b*, *c* and *sp*, and another \bar{a} , \bar{b} , \bar{c} and *sp* as shown in Fig. 3. We call the first group, the normal growth mode (type *n*) and the second, the reverse growth mode (type *r*) with respect to the substrate Ni atoms. Peaks are expected to appear for type-*n* and type-*r* domains and can be interpreted as shown in Fig. 3. Figures 3(a) and 3(b) show side views of two different kinds of Au(111) epitaxial growth mode on Ni(111) substrates, e.g., Au $[1\bar{1}\bar{2}]$ ||Ni $[1\bar{1}\bar{2}]$ (type *n*) and Au $[\bar{1}\bar{1}\bar{2}]$ ||Ni $[1\bar{1}\bar{2}]$ (type *r*). In other words, each of the films of type *n* and type *r* has a parallel and an antiparallel orientation (a lattice orientation rotated 180°) with respect to the Ni substrate. The symbol *sp* indicates the signals coming from the first layer of Au atoms (surface peak). Other symbols shown by *a* and \bar{a} indicate signals coming from the second-layer Au atoms in the normal and the reverse growth modes, respectively. Peaks labeled *b* come from the sum of signals from the third-layer Au atoms in both modes. Other peaks shown by *c* and \bar{c} also

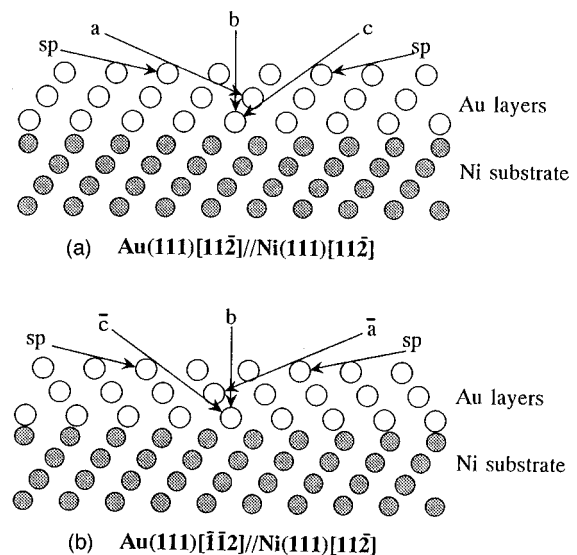


FIG. 3. Side view of the Au(111) planes heteroepitaxial growth on Ni(111) substrates. (a) and (b) shows type-*n* and type-*r* domains, respectively. The symbols *a*, *b*, *c*, *sp*, \bar{a} , and \bar{c} are positions where focusing effects are expected to appear in two different kinds of domains.

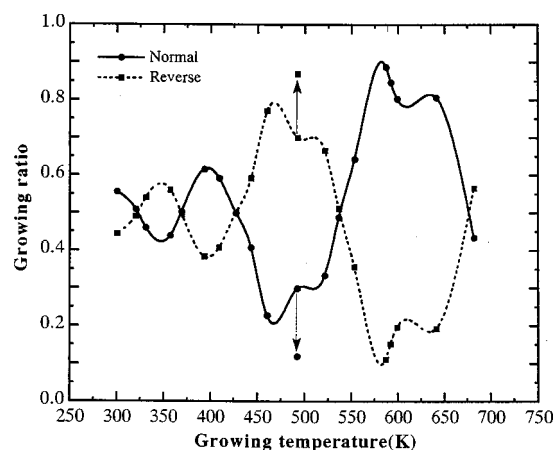


FIG. 4. Variations of growth ratio for type n and type r as a function of growth temperature during Au deposition.

come from the third-layer Au atoms in the normal and the reverse growth modes. Thus the experimental data given in Fig. 1 reveal that (a) Au(111) planes grown on the Ni substrate at 325 K have mixed domains of 50% each of type n and type r , (b) mixed domains of around 20% of type n and 80% of type r at 458 K and (c) mixed domains of around 90% of type n and 10% of type r at 591 K. These experimental results show that Au(111) planes grown have a preferred orientation of either type n or type r as a function of the Ni substrate temperature during deposition. As already shown in Fig. 2, the experimental polar scans were fitted with linear combinations of simulated scans for the two growth modes. This fit shows that there are no other significant overlayer structures present. The growing ratio determined by these fits are shown as a function of substrate temperature during the deposition in Fig. 4. This figure shows that there exist four different oscillation modes in the growth temperature range between 321 and 675 K; I (321–370 K), II (370–425 K), III (425–537 K), and IV (537–675 K). Temperature intervals of each oscillation mode becomes wider, and the amplitude becomes larger and clearer as the growing temperature increases. Each oscillation mode has similar be-

havior. One can see that the Au(111) planes grow as mixed domains of 50% each of type n and type r at specific growth temperatures of 321, 370, 425, 537, and 675 K. In practice, the ICISS spectra of polar angle scans were identical at these temperatures to that already shown in Fig. 1(a). In the first and the third oscillation modes, Au(111) planes grown on the substrate have a preferred orientation of type- r domains. On the other hand, the type- n domain is preferred as a growth mode in the second and fourth oscillation modes. After 3 ML of Au atoms were grown with a preferred orientation at a certain substrate temperature, the ratio of growth mode was frozen and independent of subsequent changes in substrate temperatures. However, when 2 ML of Au atoms were deposited at 458 K and then the annealing temperature was increased at 591 K, the growth mode changed from type r to type n . This shows that the final growth mode is controlled by the second layer of Au atoms. There is some indication that the amplitude of oscillation is dependent on the dynamics for the second-layer growth of Au atoms to seek preferred sites. This is indicated by an observation that the amplitude of the oscillations at lower temperatures is increased if the deposition is reduced to 0.04 ML/min as shown by arrows in Fig. 4. This also may explain why the observed oscillation amplitudes shown in Fig. 4 increase with deposition temperature. The mechanism underlying this dramatic oscillation behavior is not understood. Indeed, it will be important to see if similar behavior is exhibited by other heteroepitaxial systems.

In summary, we have investigated that the growth of three monolayers of Au on Ni(111) by using TOF-ICISS. We found that two different types of epitaxial growth exist: Au[$\bar{1}\bar{1}2$] \parallel Ni[$\bar{1}\bar{1}2$] (normal mode) and Au[$\bar{1}\bar{1}2$] \parallel Ni[$11\bar{2}$] (reverse mode). Growth modes of Au thin film on Ni(111) surfaces strongly depend on the growing temperature during deposition. Au(111) planes grown have a preferred orientation of either normal mode or reverse mode as a function of the Ni substrate temperature with the ratio between these modes oscillating with substrate temperatures. Furthermore, determination of the final growth mode is determined during deposition of the second ML and appears to be influenced by the deposition rate.

*Author to whom correspondence should be addressed. Electronic address: umezawa@expy.cias.osakafu-u.ac.jp

¹See reviews in *Layered Structures-Heteroepitaxy, Superlattices, Strain and Metastability*, edited by B. W. Dodson *et al.*, MRS Symposia Proceedings No. 160 (Materials Research Society, Pittsburgh, 1990).

²G. Rosenfeld, B. Poelsema, and G. Comsa, *J. Cryst. Growth* **151**, 230 (1995).

³W. Wulfhekel, I. Beckmann, N. N. Lipkin, G. Rosenfeld, B. Poelsema, and G. Comsa, *Appl. Phys. Lett.* **69**, 3492 (1996).

⁴G. Rosenfeld, R. Servaty, C. Teichert, B. Poelsema, and G. Comsa, *Phys. Rev. Lett.* **71**, 895 (1993).

⁵H. Nieuws, *Nucl. Instrum. Methods Phys. Res. B* **33**, 876 (1988).

⁶M. Aono, M. Katayama, and E. Nomura, *Nucl. Instrum. Methods Phys. Res. B* **64**, 29 (1992).

⁷R. S. Williams, M. T. Kato, R. S. Daley, and M. Aono, *Surf. Sci.* **225**, 355 (1990).

⁸S. Nakanishi, K. Kawamoto, and K. Umezawa, *Surf. Sci.* **287/**

288, 974 (1993).

⁹D. A. Andrews and D. P. Woodruff, *Surf. Sci.* **141**, 31 (1994).

¹⁰Y.-S. Ku and S. H. Overbury, *Surf. Sci.* **276**, 262 (1992).

¹¹K. Umezawa, A. Takahashi, T. Yumura, S. Nakanishi, and W. M. Gibson, *Surf. Sci.* **365**, 118 (1996).

¹²K. Umezawa, S. Nakanishi, T. Yumura, W. M. Gibson, M. Watanabe, Y. Kido, S. Yamamoto, Y. Aoki, and H. Naramoto, *Phys. Rev. B* **56**, 10 585 (1997).

¹³W. M. Yang, T. Tsakalakos, and J. E. Hilliard, *J. Appl. Phys.* **48**, 876 (1977).

¹⁴N. Nakayama, L. Wu, H. Dohonomae, T. Shinjo, J. Kim, and C. M. Falco, *J. Magn. Magn. Mater.* **126**, 71 (1993).

¹⁵J. Jacobsen, L. P. Nielsen, F. Besenbacher, I. Stensgaard, E. Lægsgaard, T. Ramussen, K. W. Jacobsen, and J. K. Nørskov, *Phys. Rev. Lett.* **75**, 489 (1995).

¹⁶L. Pleth Nielsen, F. Besenbacher, I. Stensgaard, E. Lægsgaard, C. Engdahl, P. Stoltze, K. W. Jacobsen, and J. K. Nørskov, *Phys. Rev. Lett.* **71**, 754 (1993).